



**HAL**  
open science

## Expanding the color palette of bicolor-emitting nanocrystals

Corentin Dabard, Hong Po, Ningyuan Fu, Lina Makke, Henri Lehouelleur,  
Leonardo Curti, Xu Xiangzhen, Emmanuel Lhuillier, Benjamin Diroll,  
Sandrine Ithurria

► **To cite this version:**

Corentin Dabard, Hong Po, Ningyuan Fu, Lina Makke, Henri Lehouelleur, et al.. Expanding the color palette of bicolor-emitting nanocrystals. *Nanoscale*, inPress, 10.1039/D3NR03235C . hal-04183472

**HAL Id: hal-04183472**

**<https://hal.science/hal-04183472>**

Submitted on 19 Aug 2023

**HAL** is a multi-disciplinary open access archive for the deposit and dissemination of scientific research documents, whether they are published or not. The documents may come from teaching and research institutions in France or abroad, or from public or private research centers.

L'archive ouverte pluridisciplinaire **HAL**, est destinée au dépôt et à la diffusion de documents scientifiques de niveau recherche, publiés ou non, émanant des établissements d'enseignement et de recherche français ou étrangers, des laboratoires publics ou privés.

# Expanding the color palette of bicolour-emitting nanocrystals

Corentin Dabard<sup>1</sup>, Hong Po<sup>1</sup>, Ningyuan Fu<sup>1</sup>, Lina Makke<sup>1</sup>, Henri Lehouelleur<sup>1</sup>, Leonardo Curti<sup>1</sup>, Xiang Zhen Xu<sup>1</sup>, Emmanuel Lhuillier<sup>2</sup>, Benjamin T. Diroll<sup>3</sup>, Sandrine Ithurria<sup>1\*</sup>

<sup>1</sup> Laboratoire de Physique et d'Etude des Matériaux, ESPCI-Paris, PSL Research University, Sorbonne Université Univ Paris 06, CNRS UMR 8213, 10 rue Vauquelin 75005 Paris, France.

<sup>2</sup> Sorbonne Université, CNRS, Institut des NanoSciences de Paris, INSP, F-75005 Paris, France.

<sup>3</sup> Center for Nanoscale Materials, Argonne National Laboratory, 9700 S. Cass Avenue, Lemont, Illinois 60439, United States

**Abstract:** Thanks to their bright and tunable luminescence spectra, nanocrystals appear as a unique playground for light source design. Displays and lightings require white light sources that combine several narrow lines. As Kasha's rule prevents the emission of hot carriers, blends of multiple nanocrystals populations are currently the evident strategy for broad band source design. However, a few reports suggest that bicolour emission can also be obtained from a single particle even under weak excitation, if a careful design of the exciton scattering mechanism sufficiently slows down its relaxation pathways. A key challenge remains to maintain quantum confinement for color tunability in the same structure, while simultaneously achieving a large size to leverage the critical, slower exciton diffusion or relaxation down to the ground state. Here, we demonstrate that 2D nanoplatelets offer an original opportunity for the design of confined and yet large heterostructures. We demonstrate that bicolour emission is not limited to green-red pair and show that blue-yellow as well as purple-green emissions, can be obtained respectively from CdSe/CdTe/CdSe core/crown/crown and CdSe/CdS core/crown heterostructures.

**Keywords:** nanoplatelets, photoluminescence, bicolour emission, optical spectroscopy

\*To whom correspondence should be sent: sandrine.ithurria@espci.fr

## INTRODUCTION

Kasha's rule<sup>1</sup> states that the radiative recombination of an emitter should occur through the lowest excited state. This empirical rule relies on the fact that radiative recombination is usually slow ( $\approx$  ns) compared to cooling (fs or ps range). As a result, emissions from hot carriers or higher excited states are usually prevented, except immediately after excitation, and contribute negligibly to photoluminescence. Therefore, current Liquid Crystal Displays (LCDs) relying on color down-conversion require two populations of emitters<sup>2</sup> (one green, one red) to convert the blue light from an InGaN diode and obtain white light. This, in addition to the development of two syntheses, also induces formulation issues to blend two populations of emitters into an optically transparent, gas insulating matrix. Thus, strategies that slow down carrier cooling are of utmost interest for the design of multicolor emissions. One established way is to provoke a charge carrier transport. Indeed, Kasha's rule has been established through observations in molecular fluorophores which are usually small molecules where wavefunctions are mostly spread over the whole system. This is no longer the case in complex semiconductor heterostructures such as quantum cascade lasers<sup>3</sup>. In such systems, the barrier involved in the cascade prevents a wavefunction delocalization over two consecutive periods enabling the emission of one photon per period. In the field of colloidal nanocrystals, bicolor emission has also been reported<sup>4-8</sup>. Like in quantum cascade structures in which emission and transport are spatially separated, the two emissions in colloidal nanocrystals generally result from spatially disjoint zones. The slow diffusion or kinetic barriers of the exciton<sup>9</sup> enables radiative recombination of different energies, in different areas of the structure. However, this comes at the cost that large nanoparticles usually exhibit an emission that spectrally matches the bulk emission. In CdSe, the material for which colloidal heterostructures design is the most advanced, it leads to a red emission<sup>4,6-8</sup> (from 600 to 700 nm), close to the bulk band gap emission around 1.7 eV ( $\approx$ 730 nm). Due to their high photoluminescence efficiency and unique ability for complex growth design, CdSe nanocrystals are excellent candidates for the design of new heterostructures that can achieve any multi or broadband emissions. In this quest for new heterostructures that can exhibit two-color<sup>10-12</sup> emission, maintaining confinement is an important step. In this sense, 2D nanoplatelets (NPLs) offer several advantages: (i) their specific growth mechanism<sup>13,14</sup> enables particularly narrow emissions, (ii) their anisotropic shape enables to combine both strong confinement within the thickness while presenting a large lateral extension, (iii) their specific colloidal growth allows the design of complex heterostructures involving multiple interfaces<sup>15-19</sup> (iv) the several post-synthetic doping techniques leading toward dopant<sup>20</sup> or trap emission<sup>21-25</sup>. Thus, NPLs expand the possibilities for the emission quantum engineering.

In this paper, we explore the design, growth and optical properties characterization of 2D colloidal emitters achieving two-color emission, beyond the green-red dual emission<sup>5,16</sup>. We explore here two strategies to obtain a blue-yellow emitter from strongly confined CdSe/CdTe/CdSe core/crown/crown NPLs and purple-green from the well-known CdSe/CdS core/crown NPLs.

## RESULTS AND DISCUSSION

Previous work relative to bicolor-emitting NPLs by Dabard *et al*<sup>6</sup> proposed to use a CdSe/CdTe/CdSe core/crown/crown NPLs with 4 monolayers (ML) thickness to achieve green and red emissions. The green emission was obtained from the CdSe band edge emission, while the red signal was the result of the type II recombination occurring at the CdSe/CdTe interface<sup>27</sup>. To reinforce the confinement in these NPLs, thinner objects can be used. Here, we explore the growth of 3 ML CdSe/CdTe/CdSe core/crown/crown NPLs, see a schematic of the targeted structure in **Figure 1a**. As thickness is reduced, the green emission of CdSe is now blue shifted around 460 nm, which matches the targeted wavelength for blue emission in displays (*i.e.* corresponding to the emission from InGaN quantum wells). Thin 3ML NPLs cores tend to have large lateral extensions which are often detrimental to their photoluminescence quantum yield. Here, we minimize the core lateral extension at around 11x9 nm<sup>2</sup>, see Figure S1. Those core-only NPLs display a photoluminescence (PL) peak at 460 nm characteristic of the 3 ML CdSe band edge emission. Then to obtain a second emission, without being limited by the material band edge, we design a type II interface through the growth of a first CdTe crown<sup>27-31</sup>, see Figure S1. The blue peak from CdSe PL disappears and is replaced by a broad yellow emission peaking at 572 nm, see **Figure 1c** and S1. At this stage of the lateral extension, NPLs now reach 25x15 nm<sup>2</sup>. To recover the blue emission, we add a second crown of CdSe. In this case, dual color emission is obtained, see **Figure 1b**, combining the yellow peak from the CdSe/CdTe interface

with the blue PL from the CdSe external crown. The magnitude of the blue band edge emission increases with the area of the external CdSe crown, see **Figure 1b** and S2. Emission at 460 nm from the CdSe confirms that the NPL thickness is maintained during the crown growth, while the lateral extension now reaches  $280 \times 40 \text{ nm}^2$ , see **Figure 1d**.

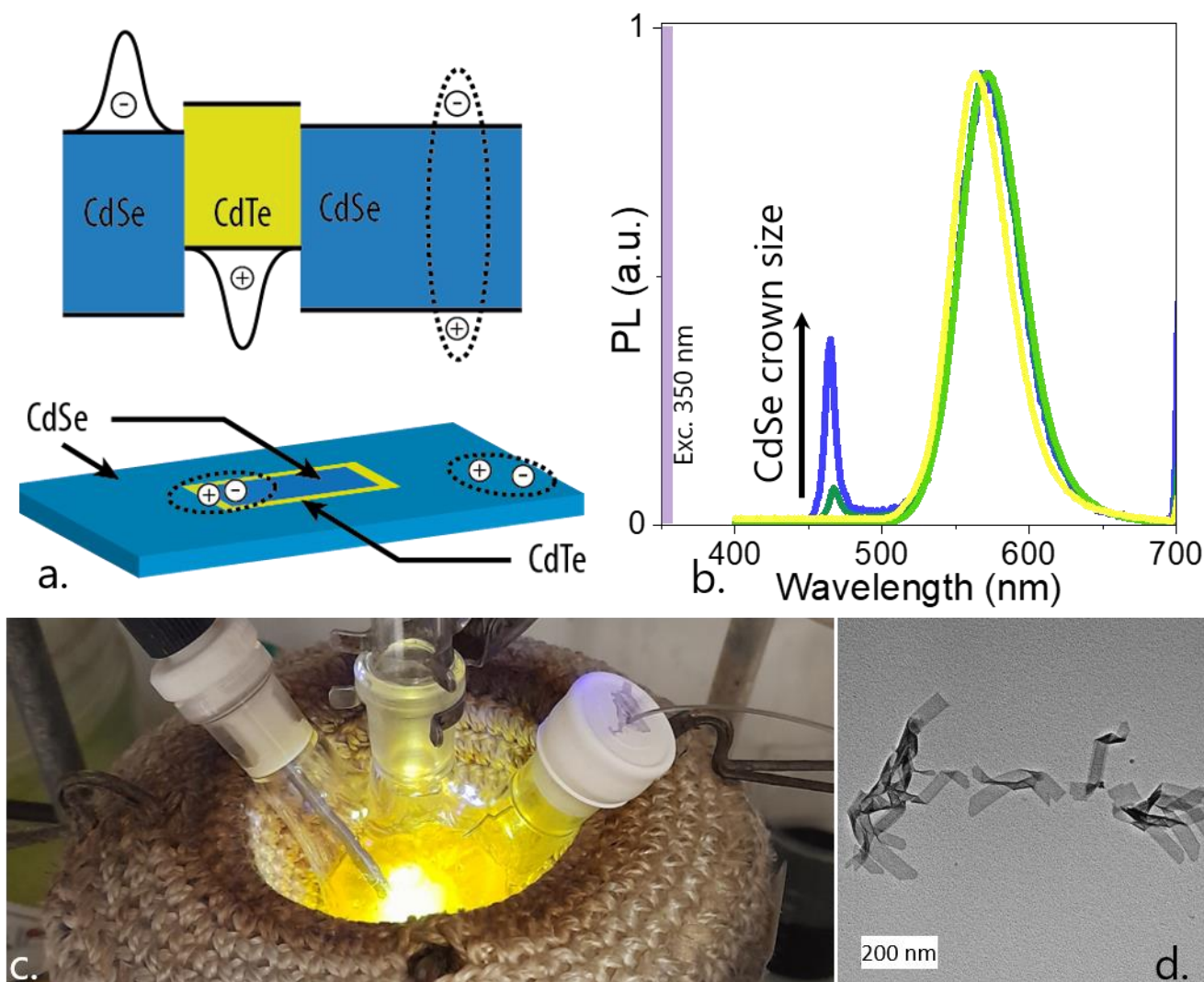


**Figure 1 Blue-yellow bicolor luminescence from 3 ML CdSe/CdTe/CdSe core/crown/crown NPLs.** a. Top schematic of the energy landscape of a CdSe/CdTe/CdSe core/crown/crown NPL as schematized in the bottom part. b. PL spectra under excitation at 350 nm at different steps of the CdSe external crown growth. c. Image of the three-neck flask containing the CdSe/CdTe/CdSe core/crown/crown NPLs excited with a 405 nm diode at the early stage of the external crown growth. d. TEM image of 3 ML CdSe/CdTe/CdSe core/crown/crown NPLs.

To understand the emission properties of these blue-yellow NPLs, we then investigate the carrier dynamics using time-resolved PL (trPL) and transient absorption (TA), see **Figure 2**. trPL reveals a much faster blue emission ( $T_{\text{blue}} = 0.65 \text{ ns}$  by fitting the decay with a single exponential), compared with the yellow emission ( $T_{\text{yellow}} = 3 \text{ ns}$ , with long component above 15 ns), see **Figure 2a**. Such difference is consistent with the type II nature of the yellow emission in which the limited spatial overlap of the electron and hole wavefunctions tends to slow down the recombination. To further confirm the type II nature of this interface, we use TA, while pumping the sample at 500 nm (*i.e.* below the CdSe band edge and resonant with CdTe band edge for 3 ML NPL). When the 500 nm pulse interacts with the sample, an AC stark effect is observed at the CdSe band edge<sup>32</sup>, with a

bleach (**Figure 2b** and c) at wavelengths corresponding to the CdSe first excitonic peak in less than 500 fs, see Figure S2 for absorption spectrum. Such bleach is associated with the electron transfer from both the CdTe and the CdTe/CdSe interface to the CdSe. When a higher energy pump is used (*i.e.* 400 nm to excite both CdSe and CdTe), see Figure S3, we have been unable to observe a distinct bleach from the charge transfer state, while this feature was observed for 4 ML NPLs. At high intensities, however, a weak and broad bleach is observed below the band gap energy of both 3 ML CdSe and CdTe NPLs, see Figure S3b. The formation of the charge transfer state being related to the exciton diffusion toward the type II interface, this process is strongly affected by the stronger confinement and may occur over a longer time scale in more confined NPLs<sup>9,33–35</sup>.

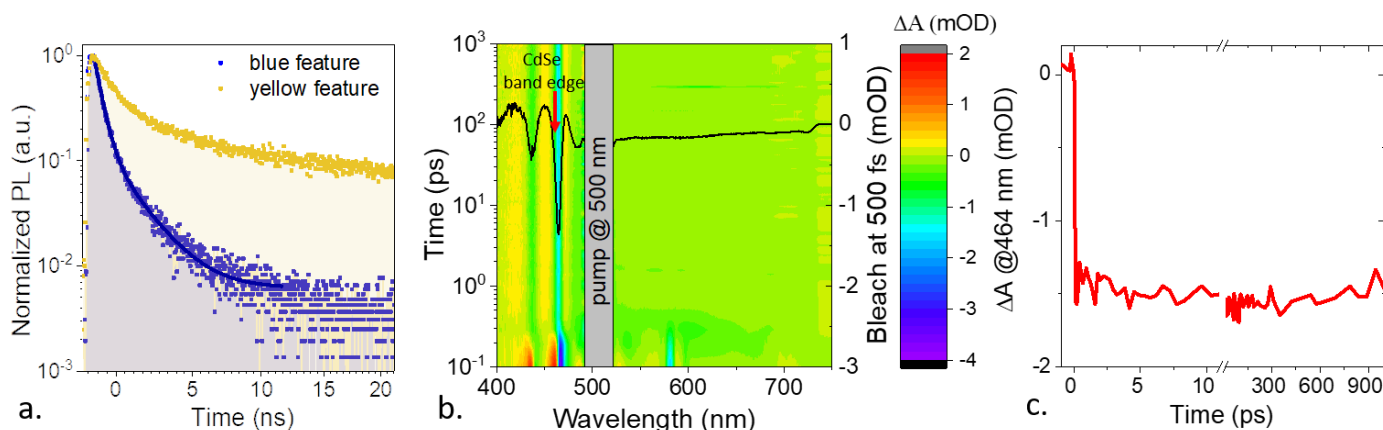


**Figure 2 Carrier dynamics in 3 ML CdSe/CdTe/CdSe core/crown/crown NPLs.** *a.* Time resolved PL signal for the blue ( $\lambda= 466$  nm) and yellow ( $\lambda= 570$  nm) features under pulsed excitation at 405 nm. *b.* Transient absorption map (*i.e.* change in absorption spectrum vs time) while the pump is at 500 nm (*i.e.* below CdSe absorption). The bleach at 500 fs is also plotted to highlight the immediate transfer to the CdSe band edge. *c.* Transient absorption at 464 nm (*i.e.* at CdSe band edge) as a function of time.

Beyond the geometrical factors (*i.e.* size of the external crown) the incident irradiance also drives the ratio of the blue-to-yellow signal, see **Figure 3**. The stronger the excitation, the more intense the blue emission. Because of this power dependent PL spectrum, the color of the solution appears strongly different as the irradiance is changed. The inset of **Figure 3a** illustrates the PL of a test tube containing a dilute solution of 3 ML CdSe/CdTe/CdSe core/crown/crown NPLs. Under UV excitation the solution appears yellow away from the focus point and blue at the focal point. It is worth pointing out that, beyond the change in the ratio of two contributions, the peaks also broaden, see **Figure 3a** and S4. The CdSe band edge emission broadens with the rise of a second contribution at lower energies. A similar feature has been observed in the case of thicker NPLs and has been attributed to the appearance of biexciton emission<sup>36</sup>. However, in the case of 3 ML NPLs, the binding energy (biexciton to exciton splitting) appears stronger (38 meV for 3 ML vs 27 meV for 4 ML in CdSe/CdTe/CdSe NPLs) which corresponds to the expected trend for the binding energy with confinement<sup>12,37</sup>. The charge transfer emission at higher fluence shows increased emission at a higher energy, a blue-shift which is consistent with a repulsive biexciton at the type II interface.

Change in emission color appears to be driven by the different scalings of the PL signal observed at various irradiance regimes. The blue PL presents a linear scaling over the irradiance range, whereas the yellow signal saturates, see **Figure 3b**. This behavior follows a similar trend to the green-red emission observed in 4ML core/crown/crown NPLs of the same composition. The blue emission mostly results from the large volume of the external CdSe crown. In fact, its large lateral

extension reduces Auger scattering whose rate scales to the inverse of the volume<sup>38,39</sup>, although scaling in NPLs is disputed<sup>37,40</sup>. On the opposite, the yellow PL is associated with the small volume of the interfaces. Thus, the Auger effect is more likely to affect the interfacial recombination leading to the observed saturation. The benefits of such bicolor emitters are better highlighted by looking at the chromaticity diagram, see **Figure 3c**. The location of the blue and yellow PL are illustrated and appear very close to what was obtained from the combination of a blue InGaN diode pumping a Ce:YAG down converter. As the power is increased, intermediate locations between the two extreme positions are obtained. In particular, a white light emission ( $x = y = 0.33$ ) can be obtained. This result will stimulate later efforts to achieve electroluminescence from such NPLs.

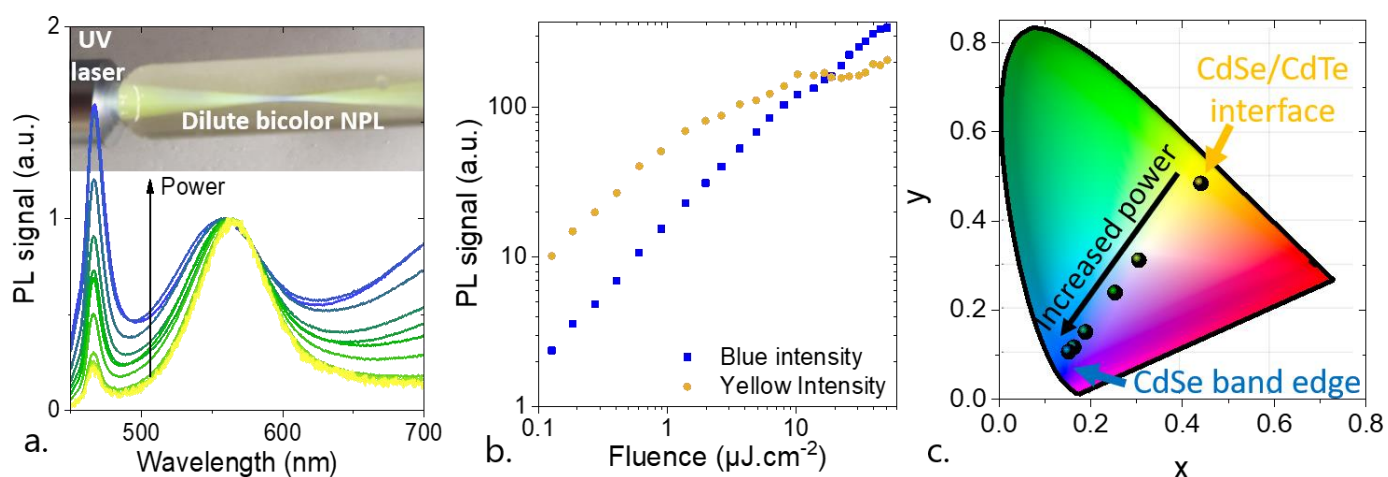


**Figure 3** Fluence dependence of the bicolor emission in 3 ML CdSe/CdTe/CdSe core/crown/crown NPLs. a. PL spectra for 3 ML CdSe/CdTe/CdSe core/crown/crown NPLs under various incident powers. The background is a picture of a test tube containing a dilute solution of NPLs excited by a UV laser. The bottom of the test tube acts as a lens, the PL color appears blue at the focal point where the excitation power is maximal, and yellow away from it. b. Blue and yellow PL signal magnitudes as a function of the incident fluence. c. Chromaticity diagram in which the blue and yellow PL signals are identified. Intermediate points corresponds to various incident excitation powers.

At this stage, NPLs appear as ideal candidates to design multicolor tunable emissions thanks to their strong confinement, while the large lateral extensions enable reduced Auger and long relaxation times. The latter point is critical to break the Kasha's rule. However, in spite of these appealing properties, solid state uses of such multicolor core/crown/crown emitters still face a major limitation, namely their low PL efficiencies under dried form. Vertical shelling with a wide band gap semiconductor (CdS, ZnS) might be a way to address this problem. However, the addition of such a shell generally comes along with a strong redshift of the emission, ruining the benefit of bicolor emission. Such redshift can be accounted when designing the bicolor emitter, thus requiring an even more confined initial emission. Another bottleneck that needs to be addressed remains the broad linewidth of the type II emission. Indeed, it will be of utmost interest to design a bicolor emitter in which both emissions result from band edge emissions. This new design rule makes worth revisiting the CdSe/CdS core/crown structure which was actually the first anisotropic heterostructure proposed for NPLs<sup>41,42</sup>. When a crown with limited lateral extension is grown around CdSe, it behaves as an exciton concentrator absorbing the high energy photons and transferring the formed exciton to the CdSe core, see Figure S5b. In this case, a single PL signal coming from the core is observed. Using our knowledge acquired on the multi-crown structure, we now consider a CdSe/CdS structure with a large external crown as schematized in **Figure 4b**. In absorption, we

notice the characteristic band edge of 4 ML CdSe NPLs at 510 nm and a strong CdS feature at 407 nm, see **Figure 4a**. The clear prevalence of the CdS signal over the features from CdSe confirms the large extension of the crown. With such a large crown, the PL displays two features corresponding to the band edge of the two components, see **Figure 4a**. It is worth pointing out that, here the two PL features are narrow (full width at half maximum of 9 nm or 67 meV for the CdS and 8 nm or, 37 meV for the CdSe). These two band-edge emissions are made possible thanks to the type I band alignment between CdSe and CdS in this heterostructure, as revealed by TA measurement in Figure S5. While the TA signal observed with a high energy pump (340 nm *i.e.* above the band edge of both materials) shows a bleach of both materials, the TA signal obtained using a 450 nm pump (*i.e.* below CdS band edge) only displays a bleach of CdSe. This result contrasts with what was observed in **Figure 2b** for the CdSe/CdTe interface in which a quasi-immediate electron transfer from CdTe to CdSe has been observed. However, similarly to the blue-yellow emitter, the irradiance can also be used as a knob to tune the ratio of the two colors, see **Figure 4c**. In this case, the higher the power, the stronger the intensity of the purple contribution. A similar scaling of the irradiance dependence of the PL peak is observed, where the PL associated with the large external crown presents linear scaling whereas the PL from the core tends to saturate, see **Figure 4d**.

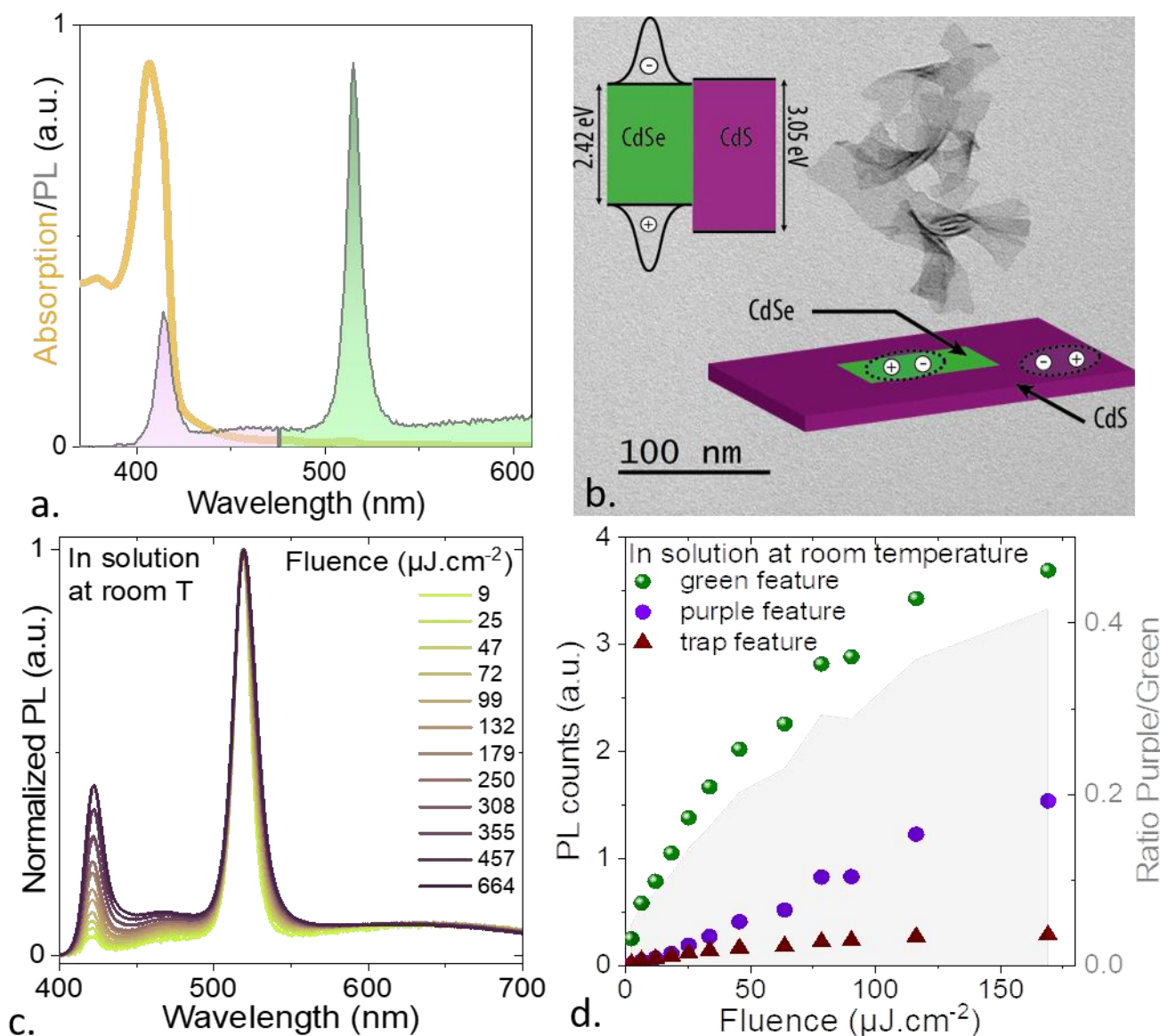


**Figure 4 Purple-green bicolor-emitting 4 ML CdSe/CdS core/crown NPLs.** a. Absorption and PL spectrum of 4 ML CdSe/CdS core/crown NPLs. b. TEM image of the 4 ML CdSe/CdS core/crown

*NPLs. Inset depicts the band alignment and structure of the 4 ML CdSe/CdS core/crown NPLs. c. PL spectra under various incident fluences at 350 nm. d. Green, purple and trap (i.e. broad feature ranging from 550 to 700 nm) PL magnitudes as a function of the incident fluence.*

## CONCLUSION

To summarize, we have designed two new types of bicolor emitters, achieving blue-yellow and purple-green emissions, respectively. The emergence of bicolor emission from a structure that has already been quite extensively studied shows that the process can be rationally designed. 2D anisotropic platforms, such as NPLs, serve as perfect building blocks for multicolor design. Future efforts should now focus on combining all three (red, green, and blue) emissions within a single particle, while also investigating the possibility to extend this concept to solid-state emitters and achieving bright electroluminescence.

## METHODS

**Chemicals:** octadecene, ODE (Sigma-Aldrich, 90 %), cadmium acetate anhydrous, Cd(OAc)<sub>2</sub> (Sigma-Aldrich, 99.995 %), cadmium oxide, CdO (Strem 99.99 %), myristic acid (Sigma-Aldrich 99 %), S powder (Sigma-Aldrich, 99.98 %), Se powder (Strem Chemicals 99.99 %), Te powder (Sigma-Aldrich 99.99 %), oleic acid, (OA, Sigma-Aldrich 90%), decanoic acid (Sigma-Aldrich, 98 %), trioctylphosphine, TOP (Alpha Aesar, 90 %), n-hexane (VWR, 99 %), ethanol (VWR, 96 %), methanol (VWR), toluene (VWR), diethyl ether (VWR), tetrahydrofuran (anhydrous, Sigma-Aldrich), isopropanol (VWR), acetone (VWR). All chemicals are used as received.

**1 M TOPTe precursor:** Te powder (2.54 g, 20 mmol) is mixed with 20 mL of TOP in a 50 mL three-neck flask. The flask is kept under vacuum at room temperature for 5 min, and after the temperature is raised to 100 °C. Degassing is conducted at this temperature for 20 min. Then, the atmosphere is switched to N<sub>2</sub> and the temperature is raised to 275 °C. The solution is stirred until a clear orange coloration is obtained. The flask is afterwards cooled down to room temperature and the color turns to yellow. Finally, this solution is transferred to a nitrogen-filled glove box for storage.

**1 M TOPSe precursor:** In a glovebox, Se powder (1.58 g, 20 mmol) is mixed with 20 mL of TOP. The mixture is stirred overnight and is stored in the glovebox for further use.

**1 M TOPS precursor:** In a glovebox, S powder (0.64 g, 20 mmol) is mixed with 20 mL of TOP. The mixture is stirred overnight and is stored in the glovebox for further use.

**Cadmium myristate (Cd(Myristate)<sub>2</sub>):** In a 50 mL three-neck flask, myristic acid (11 g, 48 mmol) and CdO (2.56 g, 20 mmol) are mixed and degassed at 80 °C for 30 min. The atmosphere is then switched to argon and the temperature is set at 200 °C. The mixture is heated until the solution becomes colorless (after about 40 min). The solution is then cooled down and 30 mL of methanol is added at 60 °C. The solid formed is washed five times by centrifugation in methanol. The final cadmium myristate is dried under vacuum at 70 °C overnight.

**Cadmium decanoate (Cd(Decanoate)<sub>2</sub>):** In a 100 mL three-neck flask, CdO (2 g, 15.6 mmol) and decanoic acid (6.9 g, 40 mmol) are mixed and heated at 210 °C for 1 h under argon atmosphere. When the entire solid is dissolved and a colorless solution is obtained, the heating is stopped and acetone is added to precipitate cadmium decanoate. The powder is centrifugated and washed at least 3 times with acetone then dried under vacuum overnight.

**Bis(stearoyl) selenide:** In a 50 mL three-neck flask, Se powder (192 mg, 2.4 mmol) is mixed with 20 mL of anhydrous tetrahydrofuran. The flask is cooled down to -10 °C using an ice bath filled with NaCl. LiAlH<sub>4</sub> (72 mg, 1.9 mmol) is swiftly added and the system is put under argon flux. A greyish color is observed. After 30 min, are added 0.68 mL of stearoyl chloride in 2 min. The operation is repeated at 60, 90, 120, and 150 min.

The color transitions from yellowish to cream to white. 25 mL of diethyl ether is added and the mixture is washed 5 times with a saturated solution of NaCl. At this point, the mixture should be brown. The mixture is heated at about 50 °C (with a heat gun) until it becomes clear, and left to recrystallize at room temperature overnight. The solid obtained is then filtered using a Büchner funnel. The solid is dried under vacuum overnight and stored in a glovebox for further use.

**3 ML CdSe NPLs synthesis:** In a 50 mL three-neck flask, Cd(Decanoate)<sub>2</sub> (68 mg, 0.15 mmol), bis(stearoyl) selenide (63 mg, 0.1 mmol), and Cd(OAc)<sub>2</sub>·2H<sub>2</sub>O (107 mg, 0.4 mmol) are mixed with 15 mL of ODE. The mixture is degassed for 1 h at room temperature. The atmosphere is then switched to argon and the temperature is set at 160 °C. The mixture is kept at this temperature for 6 h. The solution is then cooled down to room temperature and the NPLs are precipitated using toluene and a minimum amount of isopropanol. The washing is repeated two times using a minimum of isopropanol. The NPLs are redispersed in 10 mL of ODE.

**4 ML CdSe NPLs synthesis:** In a 50 mL three-neck flask, Cd(Myristate)<sub>2</sub> (340 mg, 0.6 mmol) and Se powder (24 mg, 0.3 mmol) are mixed with 25 mL of ODE. After degassing 20 min at room temperature, the atmosphere is switched to argon and the temperature is set at 230 °C. When the color turns deep orange (around 203°C), Cd(OAc)<sub>2</sub>·2H<sub>2</sub>O (110 mg, 0.4 mmol) is swiftly added. The solution is heated for 15 min more and then cooled down to room temperature. At 150 °C, OA (500 µL, 1.57 mmol) is added. Then, the obtained solution is precipitated using 20 mL of hexane and 30 mL of ethanol. The obtained pellets are redispersed in hexane and precipitated using less ethanol. The final NPLs are redispersed in 10 mL ODE.

**CdS crown in CdSe/CdS core/crown NPLs:** In a 25 mL three-neck flask, 500 µL of 4 ML CdSe NPLs (O.D.: 0.7 at 512 nm for 50 µL in 3 mL of hexane), Cd(OAc)<sub>2</sub>·2H<sub>2</sub>O (240 mg, 0.9 mmol), and OA (440 µL, 1.38 mmol) are mixed with 3 mL ODE. The mixture is degassed under vacuum at 60 °C for 1 h 30 min. The atmosphere is switched to argon and the temperature is set at 210 °C. 10 mL of a solution of TOPS in ODE (0.1 M starting from a 1 M TOPS solution) are injected at a 12 mL·h<sup>-1</sup> rate starting from 180 °C. When the temperature reaches 210 °C, the injection rate is slowed down to 2 mL·h<sup>-1</sup>. At the end of the injection, the mixture is kept at 210 °C for 10 min before cooling down to room temperature. The NPLs are precipitated twice using hexane and a minimum of ethanol. The final NPLs are redispersed in 10 mL hexane.

**CdTe crown in CdSe/CdTe core/crown NPLs:** In a 25 mL three-neck flask, 1 mL of 3 ML CdSe NPLs (O.D.: 0.22 at 460 nm for 50 µL in 3 mL of hexane), dried Cd(OAc)<sub>2</sub> (92 mg, 0.4 mmol) and OA (180 µL, 0.56 mmol) are mixed with 3 mL ODE. The mixture is degassed under vacuum at 70 °C for 1 h. The atmosphere is then switched to argon and the temperature is set at 180 °C. When the temperature stabilizes, 250 µL of a solution of TOPTe in ODE (0.005 M starting from a 1 M TOPTe solution) is injected at a 2 mL·h<sup>-1</sup> rate.

**CdSe crown in CdSe/CdTe/CdSe core/crown/crown NPLs:** After the growth of the CdTe crown, the mixture is kept at 180 °C for 10 min. The temperature is then set at 190 °C and 2 mL of a TOPSe solution (0.1 M starting from a 1 M TOPSe solution) are injected at a 2 mL·h<sup>-1</sup> rate. At the end of the injection, the mixture is cooled down to room temperature. The NPLs are precipitated twice using hexane and a minimum of ethanol.

**TEM:** For TEM imaging, a drop of diluted NPLs solution is casted on a copper grid covered with an amorphous carbon film. The grid is degassed overnight under secondary vacuum. A JEOL 2010F is used at 200 kV for the acquisition of pictures.

**Absorption spectroscopy:** UV-visible spectra were obtained with a Cary5000 spectrometer.

**Photoluminescence spectroscopy:** Photoluminescence and excitation spectra were obtained with an Edinburgh Instrument spectrometer. During the measurements, the NPLs were dispersed in hexane.

**Time resolved photoluminescence:** Time-resolved photoluminescence was collected on a colloidal dispersion in a cuvette with a 405 nm pulsed laser at 1 MHz, with emission collected into a fiber and

directed to a synchronized avalanche photodiode through a monochromator to select the wavelength of emission which was studied.

**Transient absorption:** Measurements were performed by splitting the 800 nm fundamental of a 5 kHz, 60 fs Ti: sapphire laser into pump and probe branches. The pump branch was directed through an OPA to generate various pump beams (400 nm, 500 nm) and chopped to 2.5 kHz; the probe branch was optically delayed using a variable delay stage with retroreflector and then focused into a 2 mm thick sapphire plate to generate a supercontinuum in the visible. The pump and probe pulses were spatially-overlapped at the sample position and spectra were collected by differencing pump-on and pump-off spectra.

## SUPPORTING INFORMATION

Supporting Information include details about (i) CdSe/CdTe core/crown NPLs growth and optical properties, (ii) absorption and transient absorption for 3 ML CdSe/CdTe/CdSe core/crown/crown NPLs, (iii) power dependent spectra for 3 and 4 ML CdSe/CdTe/CdSe core/crown/crown NPLs (iv) carrier dynamics in CdSe/CdS core crown NPLs.

## ACKNOWLEDGMENTS

The project is supported by ERC grants blackQD (grant n° 756225), Ne2deM (grant 853049), and AQDtive (grant n°101086358). This work was supported by French state funds managed by the Agence Nationale de la Recherche (ANR) through the grant IPER-Nano2 (ANR-18CE30-0023-01), Copin (ANR-19-CE24-0022), Frontal (ANR-19-CE09-0017), Graskop (ANR-19-CE09-0026), NITQuantum (ANR-20-ASTR-0008), Bright (ANR-21-CE24-0012), MixDFerro (ANR-21-CE09-0029) and Quicktera (ANR-22-CE09-0018). Work performed at the Center for Nanoscale Materials, a U.S. Department of Energy Office of Science User Facility, was supported by the U.S. DOE, Office of Basic Energy Sciences, under Contract No. DE-AC02-06CH11357.

## CONFLICT OF INTEREST

The authors declare no competing financial interest.

## REFERENCES

- 1 M. Kasha, *Discuss. Faraday Soc.*, 1950, **9**, 14–19.
- 2 T. Erdem and H. V. Demir, *Nanophotonics*, 2013, **2**, 57–81.
- 3 J. Faist, F. Capasso, D. L. Sivco, C. Sirtori, A. L. Hutchinson and A. Y. Cho, *Science*, 1994, **264**, 553–556.
- 4 S. Nizamoglu, E. Mutlugun, T. Özel, H. V. Demir, S. Sapra, N. Gaponik and A. Eychmüller, *Appl. Phys. Lett.*, 2008, **92**, 113110.
- 5 M. Dufour, V. Steinmetz, E. Izquierdo, T. Pons, N. Lequeux, E. Lhuillier, L. Legrand, M. Chamarro, T. Barisien and S. Ithurria, *J. Phys. Chem. C*, 2017, **121**, 24816–24823.
- 6 C. Galland, S. Brovelli, W. K. Bae, L. A. Padilha, F. Meinardi and V. I. Klimov, *Nano Lett.*, 2013, **13**, 321–328.
- 7 N. Razgoniaeva, M. Yang, C. Colegrove, N. Kholmicheva, P. Moroz, H. Eckard, A. Vore and M. Zamkov, *Chem. Mater.*, 2017, **29**, 7852–7858.
- 8 S. Brovelli, W. K. Bae, C. Galland, U. Giovanella, F. Meinardi and V. I. Klimov, *Nano Lett.*, 2014, **14**, 486–494.
- 9 Q. Li and T. Lian, *Acc. Chem. Res.*, 2019, **52**, 2684–2693.
- 10 J. Yu and R. Chen, *InfoMat*, 2020, **2**, 905–927.
- 11 M. Sharma, S. Delikanli and H. V. Demir, *Proc. IEEE*, 2020, **108**, 655–675.

- 12 B. T. Diroll, B. Guzelurk, H. Po, C. Dabard, N. Fu, L. Makke, E. Lhuillier and S. Ithurria, *Chem. Rev.*, 2023, **123**, 3543–3624.
- 13 A. Riedinger, F. D. Ott, A. Mule, S. Mazzotti, P. N. Knüsel, S. J. P. Kress, F. Prins, S. C. Erwin and D. J. Norris, *Nat. Mater.*, 2017, **16**, 743–748.
- 14 F. D. Ott, A. Riedinger, D. R. Ochsenbein, P. N. Knüsel, S. C. Erwin, M. Mazzotti and D. J. Norris, *Nano Lett.*, 2017, **17**, 6870–6877.
- 15 D. Dede, N. Taghipour, U. Quliyeva, M. Sak, Y. Kelestemur, K. Gungor and H. V. Demir, *Chem. Mater.*, 2019, **31**, 1818–1826.
- 16 A. H. Khan, G. H. V. Bertrand, A. Teitelboim, C. Sekhar M., A. Polovitsyn, R. Brescia, J. Planelles, J. I. Climente, D. Oron and I. Moreels, *ACS Nano*, 2020, **14**, 4206–4215.
- 17 S. Delikanli, B. Canimkurbey, P. L. Hernández-Martínez, F. Shabani, A. T. Isik, I. Ozkan, I. Bozkaya, T. Bozkaya, F. Isik, E. G. Durmusoglu, M. Izmir, H. Akgun and H. V. Demir, *J. Am. Chem. Soc.*, DOI:10.1021/jacs.3c00999.
- 18 F. Shabani, P. L. H. Martinez, N. Shermet, H. Korkut, I. Sarpkaya, H. Dehghanpour Baruj, S. Delikanli, F. Isik, E. G. Durmusoglu and H. V. Demir, *Small*, **n/a**, 2205729.
- 19 F. Shabani, H. Dehghanpour Baruj, I. Yurdakul, S. Delikanli, N. Gheshlaghi, F. Isik, B. Liu, Y. Altintas, B. Canimkurbey and H. V. Demir, *Small*, 2022, **18**, 2106115.
- 20 R. A. Babunts, Y. A. Uspenskaya, N. G. Romanov, S. B. Orlinskii, G. V. Mamin, E. V. Shornikova, D. R. Yakovlev, M. Bayer, F. Isik, S. Shendre, S. Delikanli, H. V. Demir and P. G. Baranov, *ACS Nano*, 2023, **17**, 4474–4482.
- 21 M. Dufour, E. Izquierdo, C. Livache, B. Martinez, M. G. Silly, T. Pons, E. Lhuillier, C. Delerue and S. Ithurria, *ACS Appl. Mater. Interfaces*, 2019, **11**, 10128–10134.
- 22 A. H. Khan, V. Pinchetti, I. Tanghe, Z. Dang, B. Martín-García, Z. Hens, D. Van Thourhout, P. Geiregat, S. Brovelli and I. Moreels, *Chem. Mater.*, 2019, **31**, 1450–1459.
- 23 M. Sharma, K. Gungor, A. Yeltik, M. Olutas, B. Guzelurk, Y. Kelestemur, T. Erdem, S. Delikanli, J. R. McBride and H. V. Demir, *Adv. Mater.*, 2017, **29**, 1700821.
- 24 M. Izmir, E. G. Durmusoglu, M. Sharma, F. Shabani, F. Isik, S. Delikanli, V. K. Sharma and H. V. Demir, *J. Phys. Chem. C*, 2023, **127**, 4210–4217.
- 25 J. Yu, S. Hu, H. Gao, S. Delikanli, B. Liu, J. J. Jasieniak, M. Sharma and H. V. Demir, *Nano Lett.*, 2022, **22**, 10224–10231.
- 26 C. Dabard, V. Guilloux, C. Gréboval, H. Po, L. Makke, N. Fu, X. Z. Xu, M. G. Silly, G. Patriarche, E. Lhuillier, T. Barisien, J. I. Climente, B. T. Diroll and S. Ithurria, *Nat. Commun.*, 2022, **13**, 5094.
- 27 A. V. Antanovich, A. V. Prudnikau, D. Melnikau, Y. P. Rakovich, A. Chuvilin, U. Woggon, A. W. Achtstein and M. V. Artemyev, *Nanoscale*, 2015, **7**, 8084–8092.
- 28 S. Pedetti, S. Ithurria, H. Heuclin, G. Patriarche and B. Dubertret, *J. Am. Chem. Soc.*, 2014, **136**, 16430–16438.
- 29 V. Steinmetz, J. I. Climente, R. Pandya, J. Planelles, F. Margailan, Y. Puttisong, M. Dufour, S. Ithurria, A. Sharma, G. Lakhwani, L. Legrand, F. Bernardot, C. Testelin, M. Chamarro, A. W. Chin, A. Rao and T. Barisien, *J. Phys. Chem. C*, 2020, **124**, 17352–17363.
- 30 Q. Li, Z. Xu, J. R. McBride and T. Lian, *ACS Nano*, 2017, **11**, 2545–2553.
- 31 R. Scott, S. Kickhöfel, O. Schoeps, A. Antanovich, A. Prudnikau, A. Chuvilin, U. Woggon, M. Artemyev and A. W. Achtstein, *Phys. Chem. Chem. Phys.*, 2016, **18**, 3197–3203.
- 32 B. T. Diroll, *Nano Lett.*, 2020, **20**, 7889–7895.
- 33 A. W. Achtstein, S. Ayari, S. Helmrich, M. T. Quick, N. Owschimikow, S. Jaziri and U. Woggon, *Nanoscale*, 2020, **12**, 23521–23531.
- 34 A. A. Kurilovich, V. N. Mantsevich, K. J. Stevenson, A. V. Chechkin and V. V. Palyulin, *Phys. Chem. Chem. Phys.*, 2020, **22**, 24686–24696.
- 35 Y. Meng, Y. Chen, L. Lu, Y. Ding, A. Cusano, J. A. Fan, Q. Hu, K. Wang, Z. Xie, Z. Liu, Y. Yang, Q. Liu, M. Gong, Q. Xiao, S. Sun, M. Zhang, X. Yuan and X. Ni, *Light Sci. Appl.*, 2021, **10**, 235.
- 36 A. Brumberg, N. E. Watkins, B. T. Diroll and R. D. Schaller, *Nano Lett.*, 2022, **22**, 6997–7004.
- 37 Q. Li and T. Lian, *Nano Lett.*, 2017, **17**, 3152–3158.
- 38 V. I. Klimov, A. A. Mikhailovsky, D. W. McBranch, C. A. Leatherdale and M. G. Bawendi, *Science*, 2000, **287**, 1011–1013.

- 39 I. Robel, R. Gresback, U. Kortshagen, R. D. Schaller and V. I. Klimov, *Phys. Rev. Lett.*, 2009, **102**, 177404.
- 40 J. P. Philbin, A. Brumberg, B. T. Diroll, W. Cho, D. V. Talapin, R. D. Schaller and E. Rabani, *J. Chem. Phys.*, 2020, **153**, 054104.
- 41 M. D. Tessier, P. Spinicelli, D. Dupont, G. Patriarche, S. Ithurria and B. Dubertret, *Nano Lett.*, 2014, **14**, 207–213.
- 42 A. Prudnikau, A. Chuvilin and M. Artemyev, *J. Am. Chem. Soc.*, 2013, **135**, 14476–14479.

# TOC graphic

